

# Grinding-induced functionalization of carbon-encapsulated iron nanoparticles

## Electronic Supplementary Information (ESI)

Artur Kasprzak,<sup>a\*</sup> Michał Bystrzejewski<sup>b</sup>, Mariola Koszytkowska-Stawinska<sup>a</sup>  
and Magdalena Poplawska<sup>a</sup>

<sup>a</sup> Faculty of Chemistry, Warsaw University of Technology, 00-664 Warsaw, Poland

<sup>b</sup> Department of Chemistry, University of Warsaw, 02-093 Warsaw, Poland

E-mail: akasprzak@ch.pw.edu.pl

### Table of contents

1. Experimental section .....	2
1.1. Materials and methods .....	2
1.2. Synthesis of the oximes.....	4
1.3. Cycloaddition reactions with graphene-encapsulated iron nanoparticles .....	8
2. NMR spectra.....	10
3. FT-IR spectra.....	15
4. TGA curves.....	20
5. XPS analyses – survey spectra .....	23
6. TEM images .....	26

# 1. Experimental section

## 1.1. Materials and methods

Carbon-encapsulated iron nanoparticles (CEINs) were synthesized by the carbon-arc route. The protocol is described in detail elsewhere.<sup>1</sup>

Ferrocenecarboxaldehyde (98%), 4-hydroxybenzaldehyde (98%), 4-carboxybenzaldehyde (97%), *N*-chlorosuccinimide (98%) were purchased from Sigma-Aldrich. D-(+)-mannose (>99%) and 2,4-dihydroxybenzaldehyde (>98%) were purchased from Fluka. Hydroxylamine hydrochloride (>99%), sodium hydroxide (>98%), triethylamine (>99,8%) were purchased from Avantor Performance Materials Poland S.A. All reagents were used as received without further purification.

Thermogravimetric analysis (TGA) was performed with a TA Q-50 instrument under nitrogen atmosphere and the heating rate of 10 °C min<sup>-1</sup>.

Fourier transformation infrared (FT-IR) spectra were recorded in a transmission mode with a Thermo Scientific Nicolet iS5 spectrometer with the spectral resolution of 4 cm<sup>-1</sup>. The samples were mixed with KBr and pressed in a form of pellets.

<sup>1</sup>H NMR and <sup>13</sup>C NMR spectra were recorded on a Varian NMR System spectrometer (500 MHz, 125 MHz) in DMSO-d<sub>6</sub> (with calibration on the residual peak 2.50 ppm and 39.5 ppm, for <sup>1</sup>H NMR and <sup>13</sup>C NMR, respectively) or CDCl<sub>3</sub> (with calibration on the residual peak 7.26 ppm and 77.16 ppm, for <sup>1</sup>H NMR and <sup>13</sup>C NMR, respectively). The MestRe-C 2.0 software was used for the simulation of NMR spectra (*MestRe-C NMR Data Processing Made Easy 4.9.9.6, 1996– 2006, courtesy F.J. Sardina, Universidad de Santiago de Compostela, Spain*).

The morphological details were analyzed by transmission electron microscopy (TEM) using a Zeiss Libra Plus instrument (accelerating voltage: 120 kV).

The XPS experiments were carried out using XPS system provided by SPECS Surface Nano Analysis GmbH, Berlin, Germany, equipped with XR 50 MF X-ray source and μ-Focus 600 monochromator (600 mm Rowland Circle), using monochromatized X-ray Al K $\alpha$  emission line, photon energy 1486.6 eV, operating at 120 W, and Phoibos 150 hemispherical analyzer with 150 mm radius, NAP version, equipped with 2D-DLD detector. The system base pressure was in the 10<sup>-10</sup> mbar range. Spectra were fitted using CasaXPS

---

<sup>1</sup> (a) M. Bystrzejewski, A. Huczko and H. Lange, *Sens. Actuators B*, 2005, **109**, 81-85; (b) J. Borysiuk, A. Grabias, J. Szczytko, M. Bystrzejewski, A. Twardowski and H. Lange, *Carbon*, 2008, **46**, 1693-1701.

software, version 2.3.17PR1.1 and the quantitative analysis were performed using CasaXPS built-in Scofield relative sensitivity factors.

Sonication of carbon materials was performed using a Bandelin Sonorex RK 100 H ultrasonic probe (ultrasonic peak output/HF power: 320W/80W; 35 kHz).

## 1.2 Synthesis of the oximes

*Synthesis of 4-carboxybenzaldehyde oxime, 4-hydroxybenzaldehyde oxime, ferrocenecarboxaldehyde oxime, 2,4-dihydroxybenzaldehyde oxime*

Aldehyde (6.0 mmol) and hydroxylamine hydrochloride (7.2 mmol) were placed in an agate mortar and ground together with an agate pestle. Solid sodium hydroxide (7.2 mmol) was then added and the mixture was ground further for 5 min at room temperature with the addition of 1 drop of methanol. The reaction mixture was left for 5 minutes, then ground for another 5 min with the addition of 1 drop of methanol. 4-Carboxybenzaldehyde, 4-hydroxybenzaldehyde, 2,4-dihydroxybenzaldehyde) were isolated by washing of the crude mixture with diethyl ether. All impurities were undissolved. Ethyl acetate was used to isolate ferrocenecarboxaldehyde oxime. Finally, solvent was evaporated and the product was dried under high vacuum. The yields of the products were as follows:

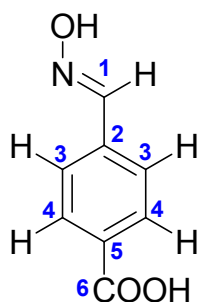
- 4-carboxybenzaldehyde oxime: 96%,
- 4-hydroxybenzaldehyde oxime: 96%,
- 2,4-dihydroxybenzaldehyde oxime: 96%,
- ferrocenecarboxaldehyde oxime: 95%.

The full conversion of the examined aldehydes into the corresponding oximes was confirmed by the  $^1\text{H}$  and  $^{13}\text{C}$  NMR spectra. The existence of the oximes in the format of (E)-isomers was confirmed by a comparison of the recorded NMR spectra with those reported in the literature.<sup>2</sup>

---

<sup>2</sup> For 4-carboxybenzaldehyde oxime: J. Yang, M. Puchberger, R. Qian, C. Maurer and U. Schubert, *Eur. J. Inorg. Chem.*, 2012, **27**, 4294-4300; for 4-hydroxybenzaldehyde oxime: J. Yu, Y. Jin and M. Lu, *Adv. Synth. Catal.*, 2015, **357**, 1175–1180; for 2,4-dihydroxybenzaldehyde oxime: (a) Y. Xu, X. Yin, Y. Huang, P. Du and B. Zhang, *Chem. Eur. J.*, 2015, **21**, 4571–4575, (b) A. Tarai and J. B. Baruah, *CrystEngComm*, 2015, **17**, 2301-2309; for ferrocenecarboxaldehyde oxime: Y. Wang, A. Rapakousiou, C. Latouche, J.-C. Daran, A. Singh, I. Ledoux-Rak, J. Ruiz, J.-Y. Saillard and D. Astruc, *Chem. Commun.*, 2013, **49**, 5862-5864.

#### 4-carboxybenzaldoxime:

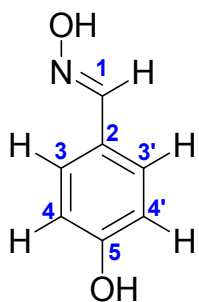


$^1\text{H NMR}$   $\delta_{\text{H}}$  (500 MHz, DMSO- $d_6$ , ppm): 12.95 (bs, 1H, COOH), 11.55 (bs, 1H, N-OH), 8.20 (s, 1H, **H-1**), 7.96 (m, AA'BB',  $J_{\text{AB}} = 7.9$  Hz, 2H, **H-4,4'**), 7.71 (m, AA'BB',  $J_{\text{BA}} = 7.9$  Hz, 2H, **H-3,3'**)

$^{13}\text{C NMR}$   $\delta_{\text{C}}$  (125 MHz, DMSO- $d_6$ , ppm): 166.99 (**C-6**), 147.57 (**C-1**), 137.21 (**C-5**), 131.15 (**C-2**), 129.74 (**C-3,3'**), 126.45 (**C-4,4'**)

FT-IR (KBr):  $\nu = 3200, 2650, 2545, 1690, 1615, 1425, 1290, 1000, 870, 780, 700, 535$   $\text{cm}^{-1}$

#### 4-hydroxybenzaldoxime:

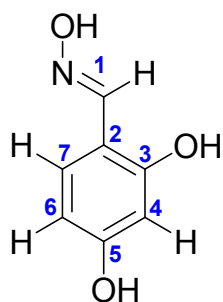


$^1\text{H NMR}$   $\delta_{\text{H}}$  (500 MHz, DMSO- $d_6$ , ppm): 10.86 (bs, 1H, OH), 9.69 (bs, 1H, N-OH), 8.03 (s, 1H, **H-1**), 7.44 (m, AA'BB',  $J_{\text{AB}} = 7.4$  Hz, 2H, **H-3,3'**), 7.0 (m, AA'BB',  $J_{\text{BA}} = 7.4$  Hz, 2H, **H-4,4'**)

$^{13}\text{C NMR}$   $\delta_{\text{C}}$  (125 MHz, DMSO- $d_6$ , ppm): 158.50 (**C-5**), 147.83 (**C-1**), 127.90 (**C-2**), 123.99 (**C-3,3'**), 115.51 (**C-4,4'**)

FT-IR (KBr):  $\nu = 3200, 2880, 2795, 1650, 1600, 1450, 1270, 1155, 830, 603$   $\text{cm}^{-1}$

### 2,4-dihydroxybenzaloxime:

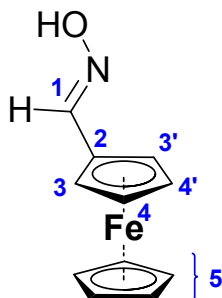


$^1\text{H NMR}$   $\delta_{\text{H}}$  (500 MHz, DMSO- $d_6$ , ppm): 10.96 (bs, 1H, OH-3), 10.12 (bs, 1H, OH-5), 9.75 (bs, 1H, N-OH), 8.21 (s, 1H, H-1), 7.24 (d,  $J = 7.2$  Hz, 1H, H-7), 6.32 (m, 2H, H-4 and H-6)

$^{13}\text{C NMR}$   $\delta_{\text{C}}$  (125 MHz, DMSO- $d_6$ , ppm): 159.68 (C-3), 157.68 (C-5), 148.34 (C-1), 129.52 (C-7), 109.75 (C-2), 107.44 (C-6), 102.41 (C-4)

FT-IR (KBr):  $\nu = 3270, 2900, 2760, 1625, 1600, 1470, 1305, 1170, 980, 830, 600$   $\text{cm}^{-1}$

### ferrocenecarboxaldehyde oxime:



$^1\text{H NMR}$   $\delta_{\text{H}}$  (500 MHz,  $\text{CDCl}_3$ , ppm): 7.97 (s, 1H, H-1), 7.76 (bs, 1H, OH), 4.52 (bm, 2H, Cp-H-3,3'), 4.35 (bm, 2H, Cp-H-4,4'), 4.52 (s, 5H, Cp-H-5),

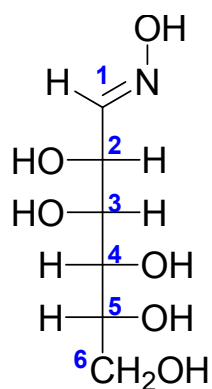
$^{13}\text{C NMR}$   $\delta_{\text{C}}$  (125 MHz,  $\text{CDCl}_3$ , ppm): 150.20 (C-1), 77.41 (Cp-C-2), 76.91 (Cp-C-3,3'), 69.35 (Cp-C-4,4' and Cp-C-5)

FT-IR (KBr):  $\nu = 3190, 2980, 2870, 1625, 1380, 1295, 1105, 1045, 970, 815, 510$   $\text{cm}^{-1}$

### Synthesis of D-mannose oxime

D-mannose (6.0 mmol) and hydroxylamine hydrochloride (7.2 mmol) were placed in an agate mortar and ground together with an agate pestle. Solid sodium hydroxide (7.2 mmol) was then added and the mixture was ground further for 5 min at room temperature with the addition of 1 drop of methanol. The reaction mixture was left for 5 minutes, then ground for another 5 min with the addition of 1 drop of methanol. The crude mixture was washed with methanol to remove the inorganic salts and the residue was air dried. to give D-mannose oxime (84%). The full conversion of the starting sugar material into the corresponding oxime was confirmed by the  $^1\text{H}$  and  $^{13}\text{C}$  NMR spectra. The existence of the oxime in the format of (E)-isomer was confirmed by a comparison of the recorded NMR spectra with those reported in the literature.<sup>3</sup>

#### D-mannose oxime:



$^1\text{H}$  NMR  $\delta_{\text{H}}$  (500 MHz, DMSO- $d_6$ , ppm): 10.51 (s, 1H, N-OH), 7.22 (d,  $J = 7.6$  Hz, 1H, **H-1**), 5.07 (d,  $J = 5.5$  Hz, 1H, **OH-5**), 4.42 (d,  $J = 5.5$  Hz, 1H, **OH-3**), 4.32 (t,  $J = 5.6$  Hz, 1H, **OH-6**), 4.26 (d,  $J = 5.6$  Hz, 1H, **OH-4**), 4.18 (d,  $J = 5.6$  Hz, 1H, **OH-2**), 4.00 (m, 1H, **H-5**), 3.62 (m, 2H, **H-3**), 3.53 (m, 2H, **CH<sub>2</sub>-6**), 3.45 (m, 1H, **H-4**), 3.39 (m, 1H, **H-2**),

$^{13}\text{C}$  NMR  $\delta_{\text{C}}$  (125 MHz, DMSO- $d_6$ , ppm): 152.02 (**C-1**), 71.46 (**C-4**), 70.87 (**C-3**), 69.64 (**C-5**), 68.79 (**C-2**), 64.04 (**C-6**)

**FT-IR** (KBr):  $\nu = 3350, 2945, 2830, 1530, 1460, 1325, 1285, 1090, 1020, 960, 800, 650$   $\text{cm}^{-1}$

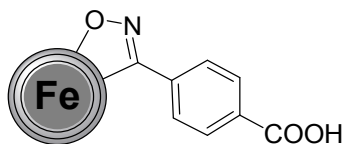
<sup>3</sup> J. Brand, T. Huhn, U. Groth and J. C. Jochims, *Chem. Eur. J.*, 2006, **12**, 499–509.

### 1.3 Cycloaddition reactions with graphene-encapsulated iron nanoparticles

Oxime (1.2 mmol), *N*-chlorosuccinimide (1.5 mmol) and CEINs (20 mg) were placed in an agate mortar and ground together with an agate pestle for 1 min. Triethylamine (140  $\mu$ L; 1.5 mmol) and pyridine (20  $\mu$ L; 0.2 mmol) were then added and the mixture was ground further for 8 min at room temperature. A small amount of acetone was added to the crude reaction mixture and the carbon nanomaterial was then separated by filtration over a nylon membrane (0.45  $\mu$ m pore size). The obtained solid was washed with water and small amount of acetone. The crude product was dispersed in 20 mL of methanol (NANO-1,2,3,4) or water (NANO-5), sonicated for 2 h, filtered off, washed with water and finally with small amount of acetone and dried in 45°C overnight. The amount of the product was as follows:

- NANO-1 (reaction with 4-carboxybenzaldoxime): 24,3 mg,
- NANO-2 (reaction with 4-hydroxybenzaldoxime): 23,0 mg,
- NANO-3 (reaction with 2,4-dihydroxybenzaldoxime): 22,1 mg,
- NANO-4 (reaction with ferrocenecarboxaldehyde): 26,2 mg,
- NANO-5 (reaction with D-mannose oxime): 22,9 mg.

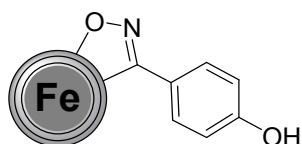
NANO-1 (reaction with 4-carboxybenzaldoxime)



FT-IR (KBr):  $\nu = 1685, 1610, 1415, 1285, 1085, 860, 760, 730, 685, 540 \text{ cm}^{-1}$

TGA (content of introduced moiety): 33.5 wt. %

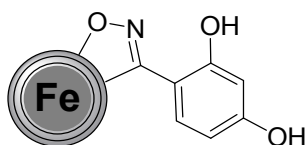
NANO-2 (reaction with 4-hydroxybenzaldoxime)



FT-IR (KBr):  $\nu = 1595, 1440, 1290, 1145, 985, 840, 700, 580, 520 \text{ cm}^{-1}$

TGA (content of introduced moiety): 23.2 wt. %

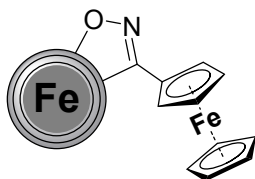
NANO-3 (reaction with 2,4-dihydroxybenzaldoxime)



**FT-IR** (KBr):  $\nu = 1590, 1505, 1275, 1185, 1100, 955, 820, 730, 595 \text{ cm}^{-1}$

**TGA** (content of introduced moiety): 21.1 wt. %

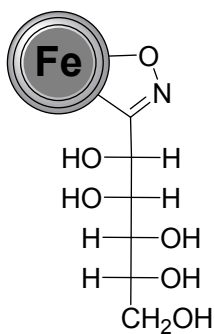
**NANO-4** (reaction with ferrocenecarboxaldehyde oxime)



**FT-IR** (KBr):  $\nu = 1630, 1540, 1415, 1295, 1260, 1095, 1005, 805, 645, 495 \text{ cm}^{-1}$

**TGA** (content of introduced moiety): 16.3 wt. %

**NANO-5** (reaction with D-mannose oxime)



**FT-IR** (KBr):  $\nu = 1480, 1460, 1330, 1200, 1100, 1050, 905, 750, 625 \text{ cm}^{-1}$

**TGA** (content of introduced moiety): 17.2 wt. %

## 2. NMR spectra

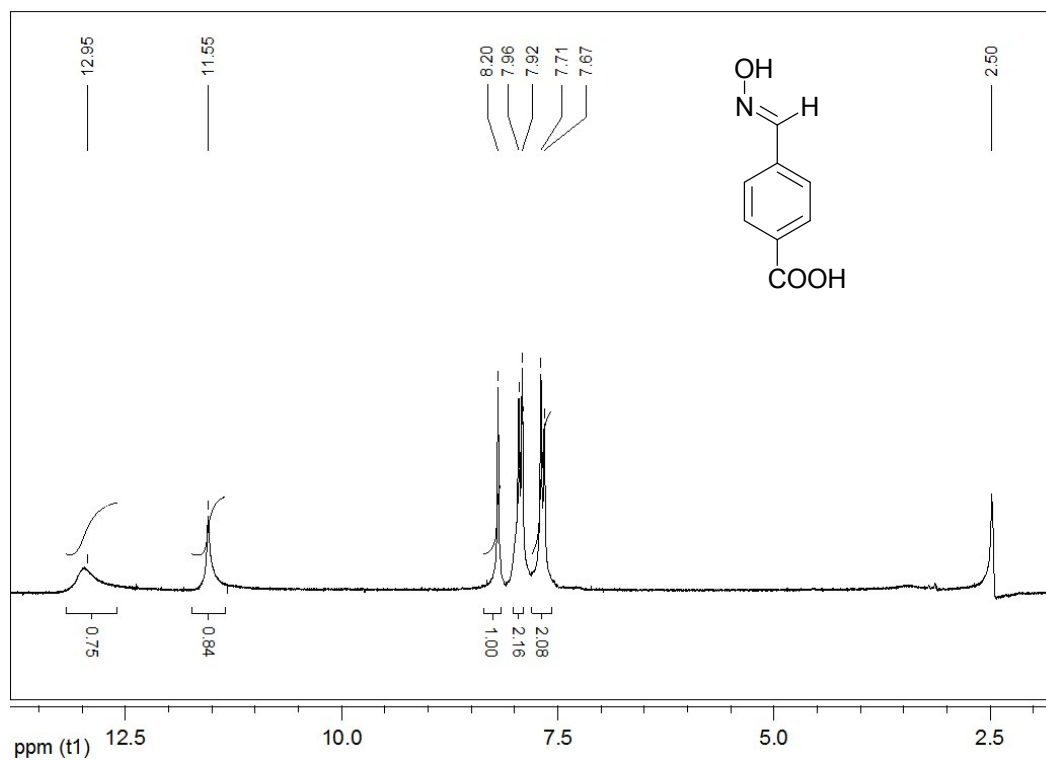


**Fig. S1.** <sup>1</sup>H NMR (500 MHz, DMSO-*d*<sub>6</sub>) of 4-carboxybenzaloxime

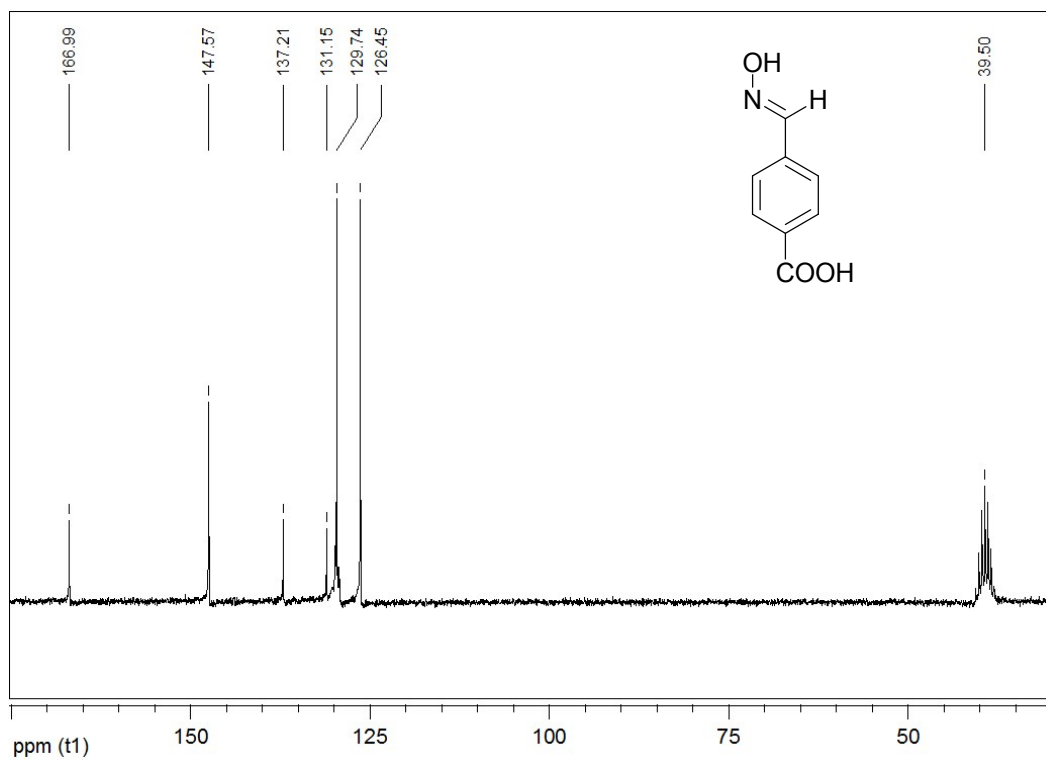


**Fig. S2.** <sup>13</sup>C NMR (125 MHz, DMSO-*d*<sub>6</sub>) of 4-carboxybenzaloxime

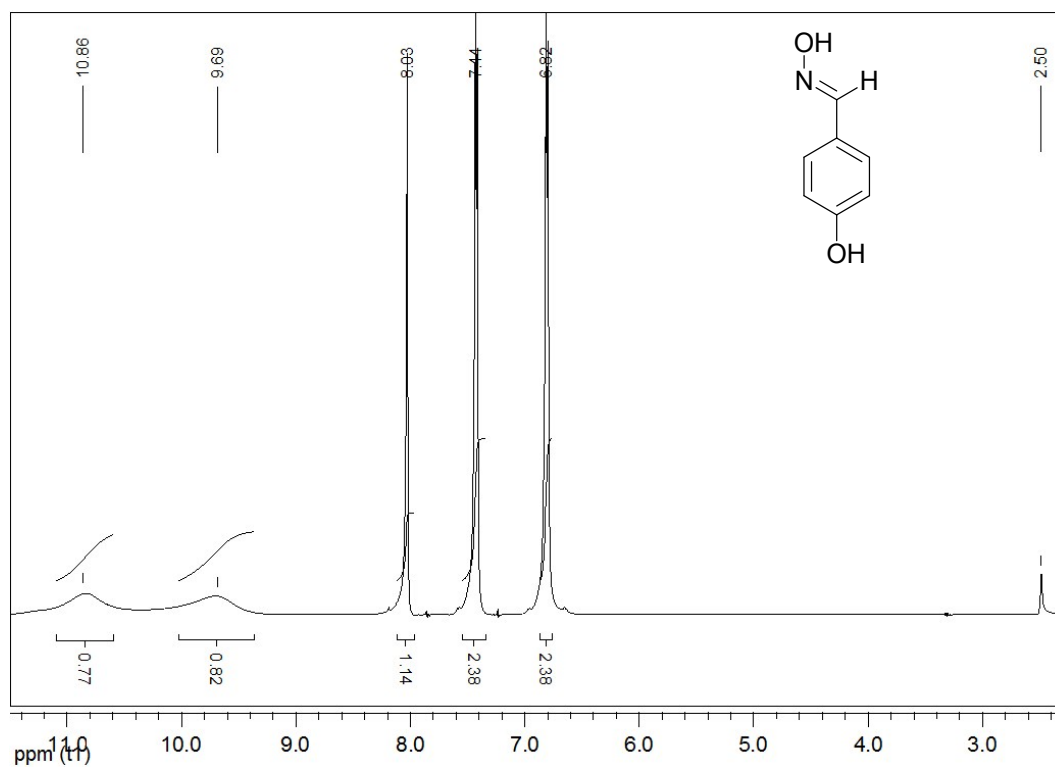


**Fig. S3.**  $^1\text{H}$  NMR (500 MHz,  $\text{DMSO-}d_6$ ) of 4-hydroxybenzaloxime

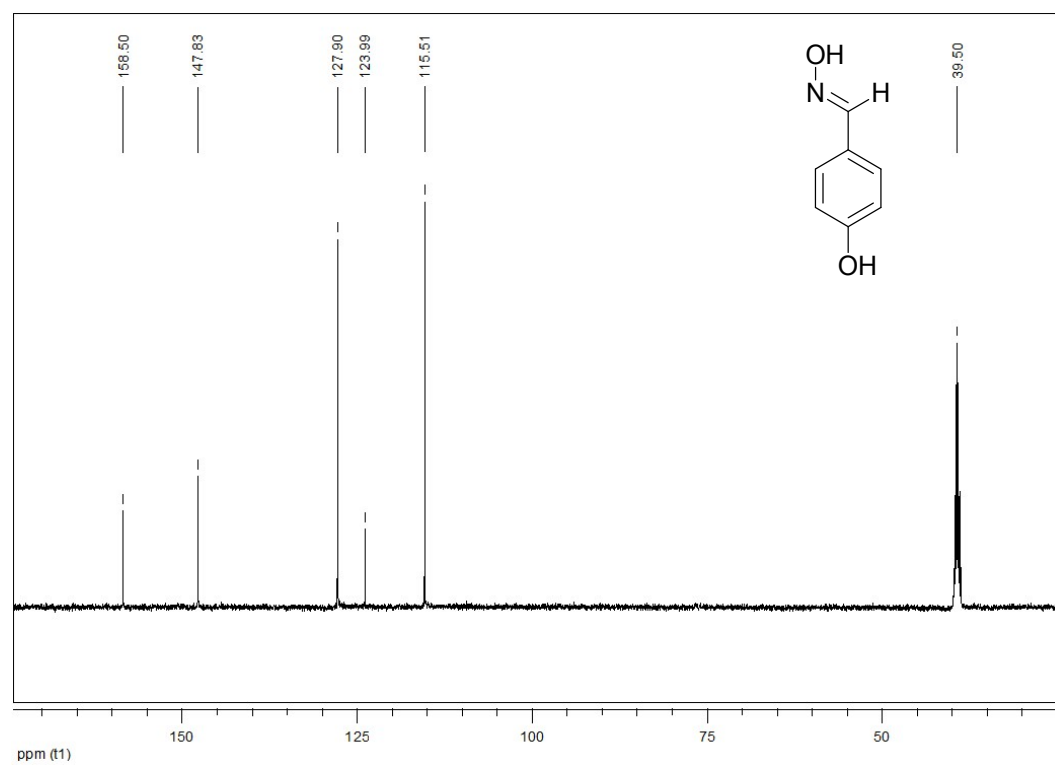


**Fig. S4.**  $^{13}\text{C}$  NMR (125 MHz,  $\text{DMSO-}d_6$ ) of 4-hydroxybenzaloxime

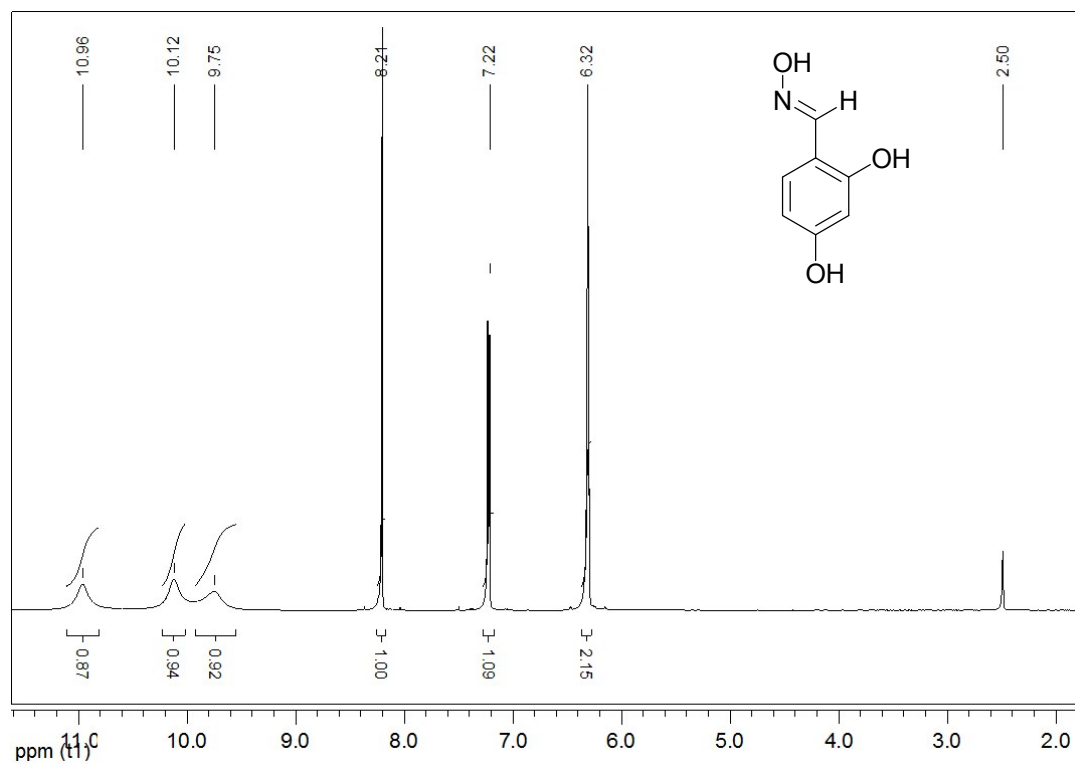


**Fig. S5.**  $^1\text{H}$  NMR (500 MHz,  $\text{DMSO-}d_6$ ) of 2,4-dihydroxybenzaloxime

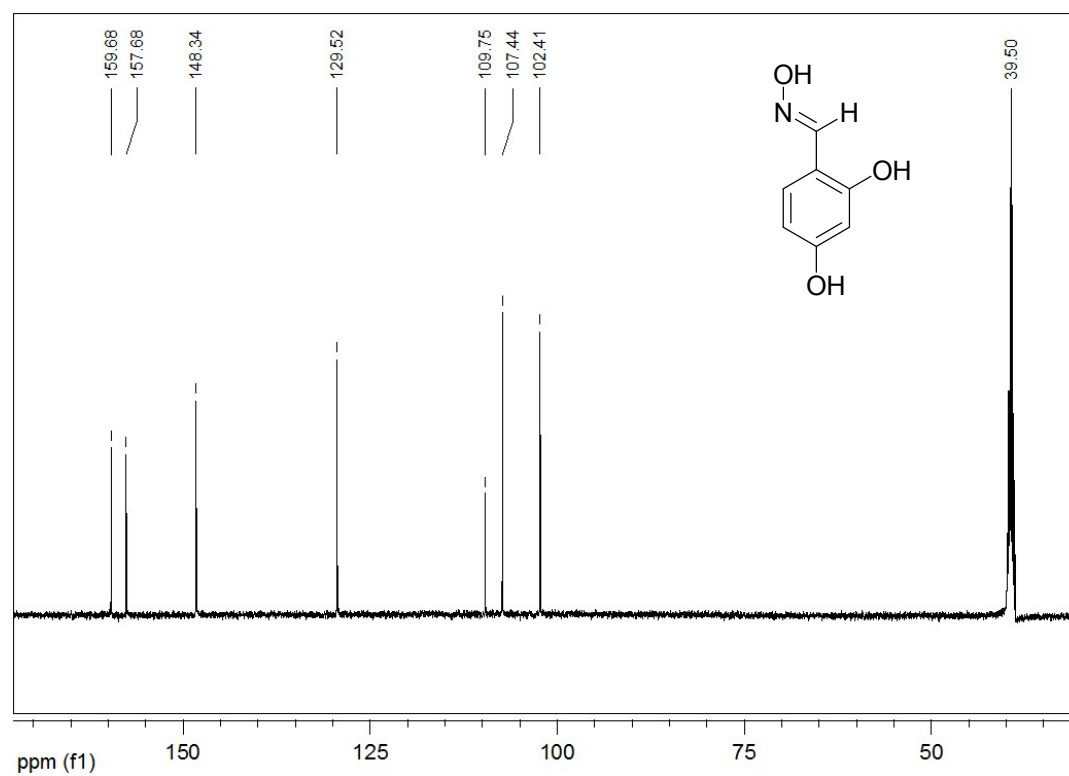


**Fig. S6.**  $^{13}\text{C}$  NMR (125 MHz,  $\text{DMSO-}d_6$ ) of 2,4-dihydroxybenzaloxime

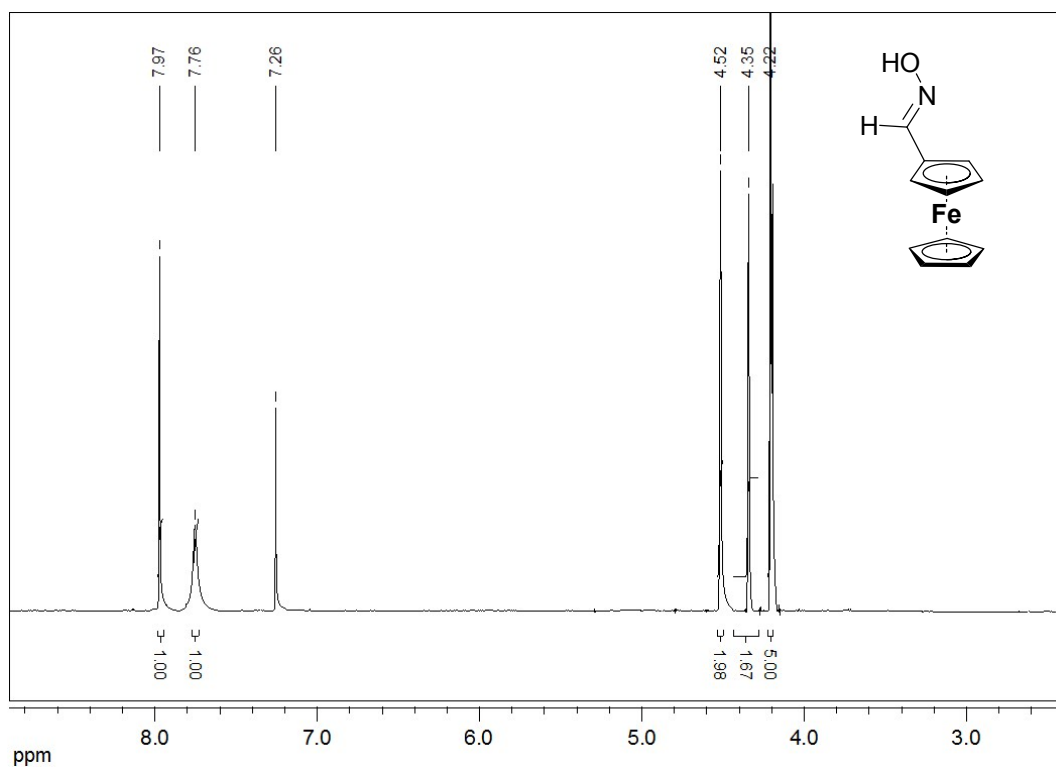


**Fig. S7.**  $^1\text{H}$  NMR (500 MHz,  $\text{CDCl}_3$ ) of ferrocenecarboxaldehyde oxime

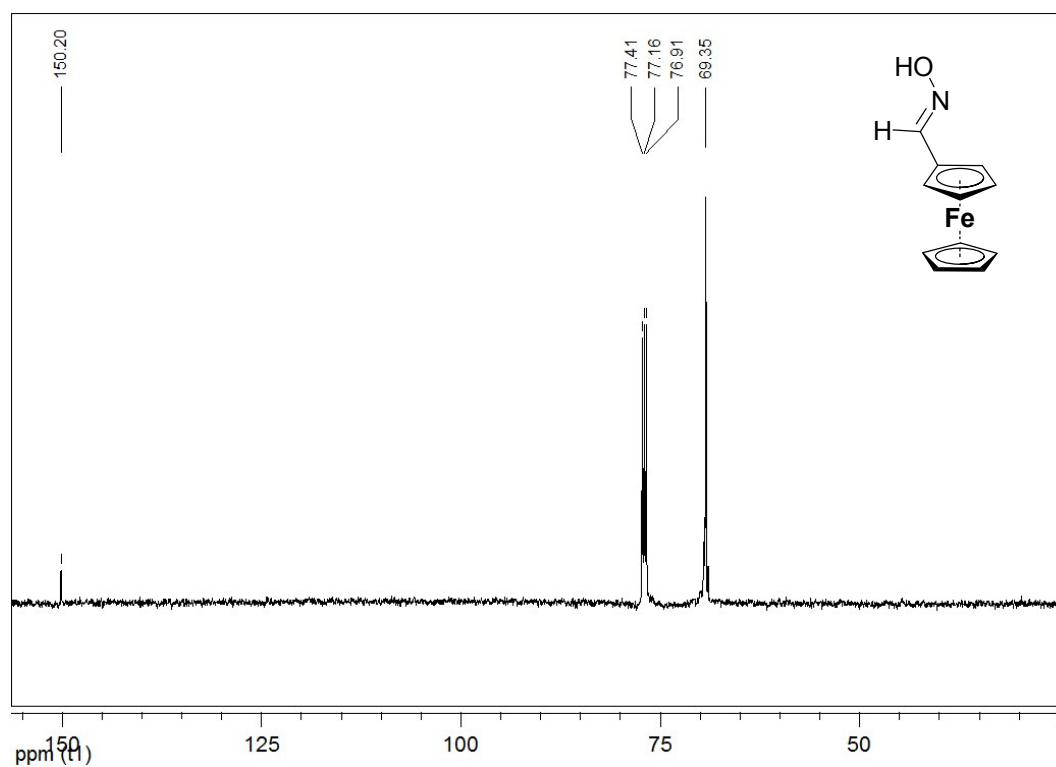


**Fig. S8.**  $^{13}\text{C}$  NMR (125 MHz,  $\text{CDCl}_3$ ) of ferrocenecarboxaldehyde oxime

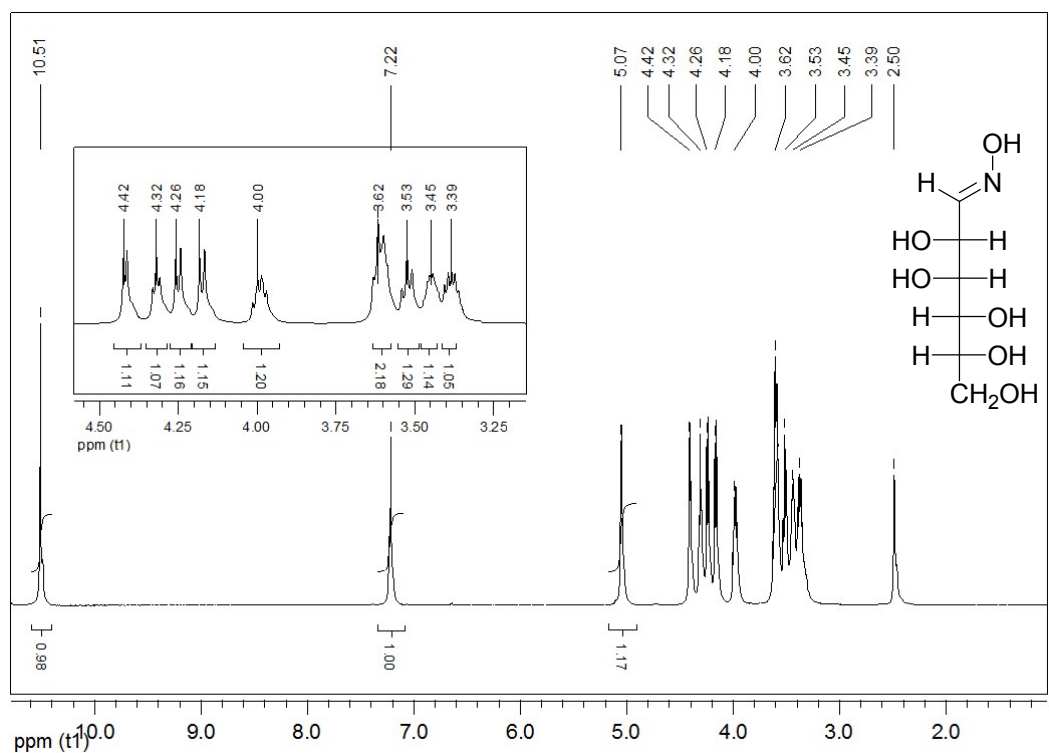


Fig. S9.  $^1\text{H}$  NMR (500 MHz,  $\text{DMSO-}d_6$ ) of D-mannose oxime

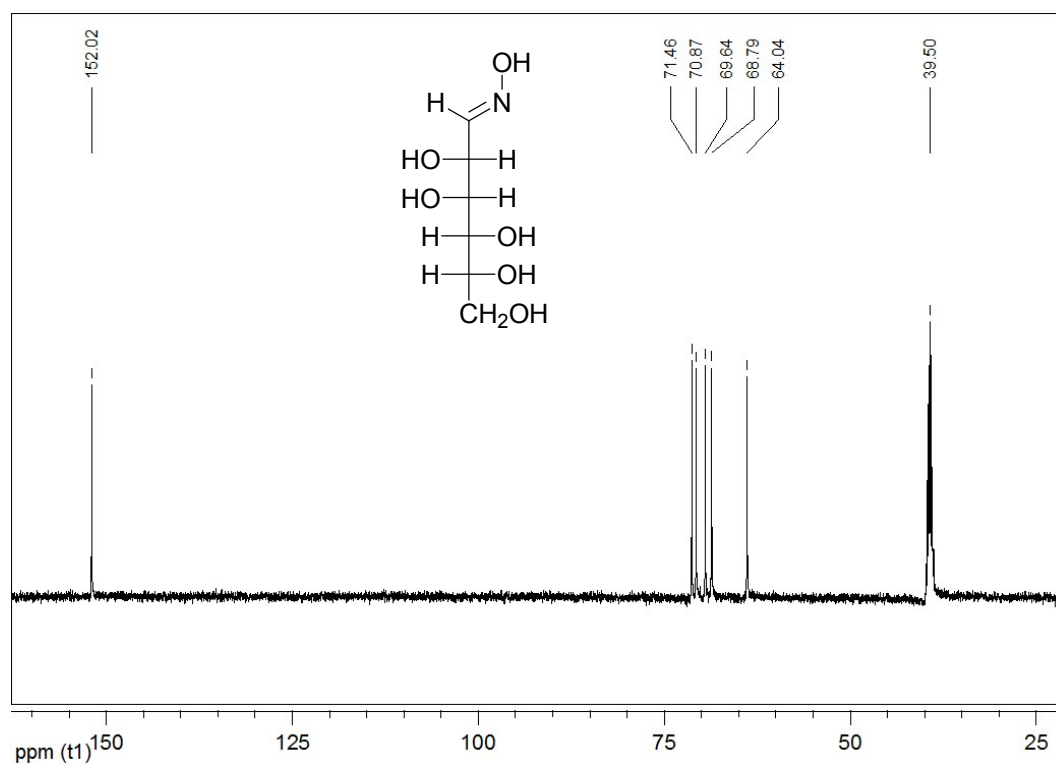


Fig. S10.  $^{13}\text{C}$  NMR (125 MHz,  $\text{DMSO-}d_6$ ) of D-mannose oxime

### 3. FT-IR spectra

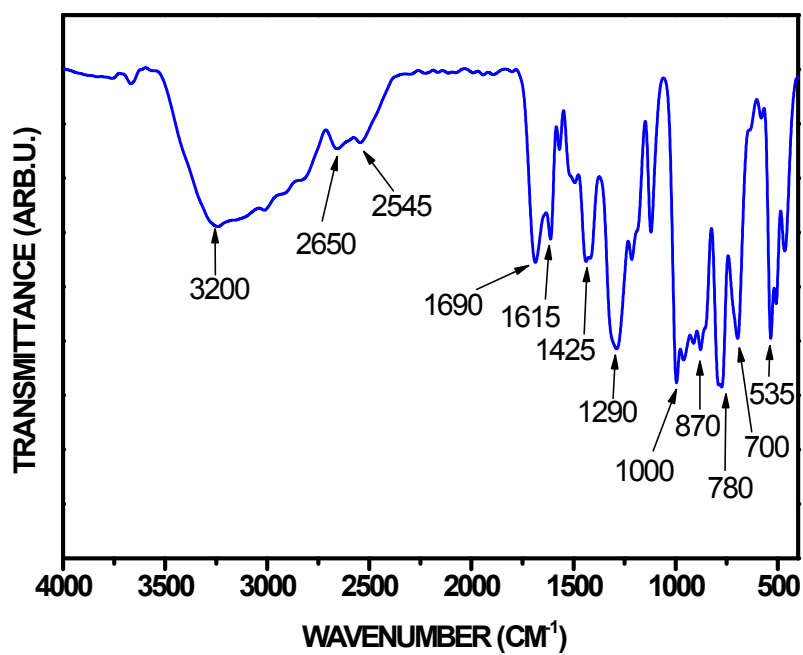


Fig. S11. FT-IR spectrum of 4-carboxybenzaloxime

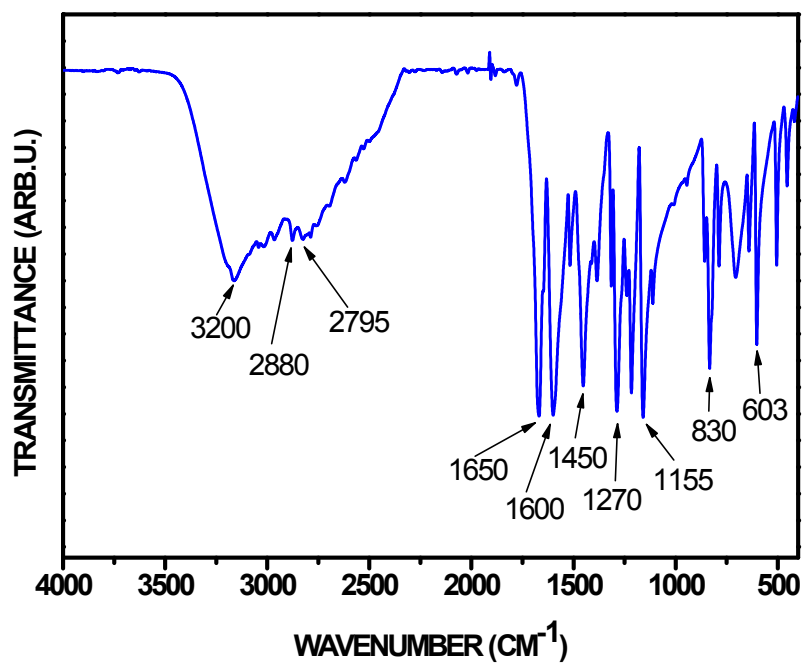


Fig. S12. FT-IR spectrum of 4-hydroxybenzaloxime

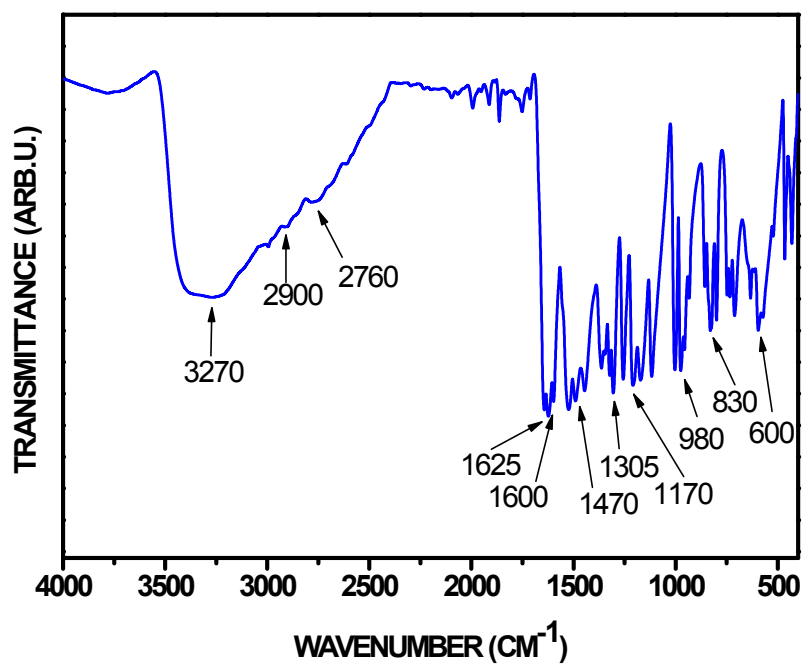


Fig. S13. FT-IR spectrum of 2,4-dihydroxybenzaloxime

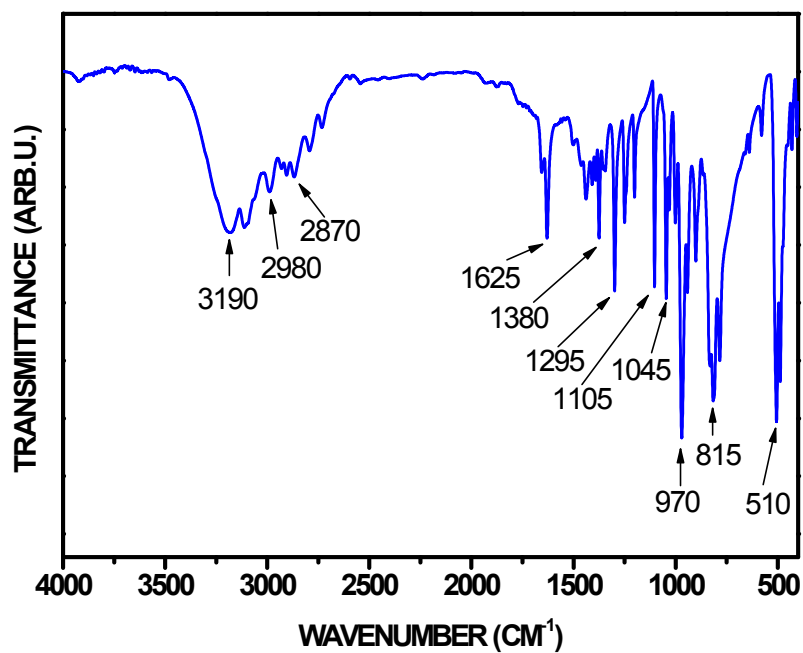


Fig. S14. FT-IR spectrum of ferrocenecarboxaldehyde oxime

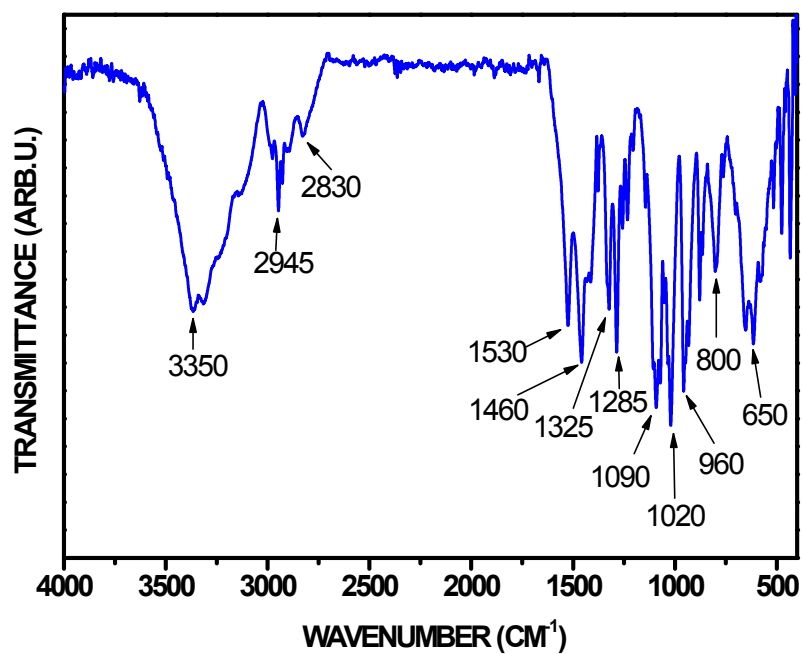


Fig. S15. FT-IR spectrum of D-mannose oxime

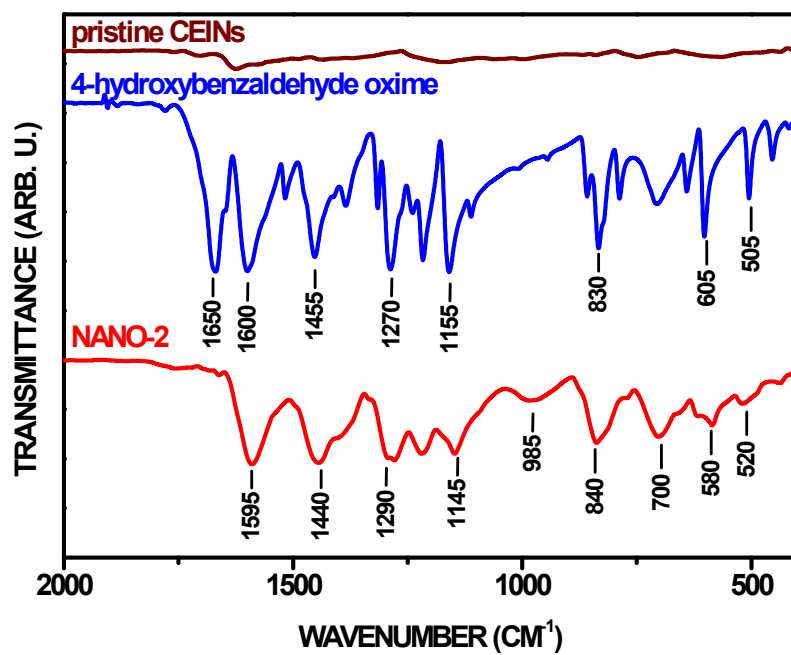


Fig. S16. FT-IR spectrum of NANO-2. FT-IR spectra of pristine CEINs and 4-hydroxybenzaldehyde oxime are also presented. For legends see subsection 1.3 in ESI

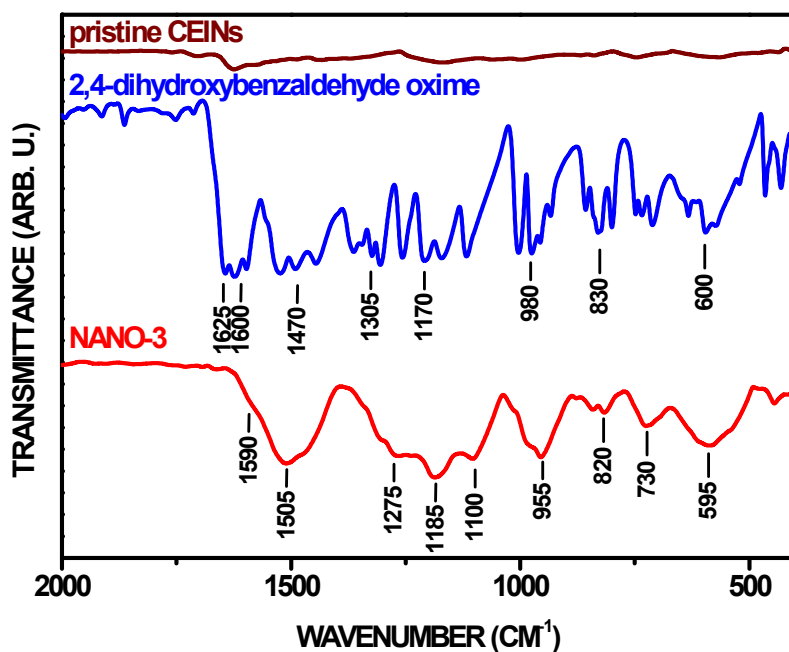


Fig. S17. FT-IR spectrum of NANO-3. FT-IR spectra of pristine CEINs and 2,4-dihydroxybenzaldehyde oxime are also presented. For legends see subsection 1.3 in ESI

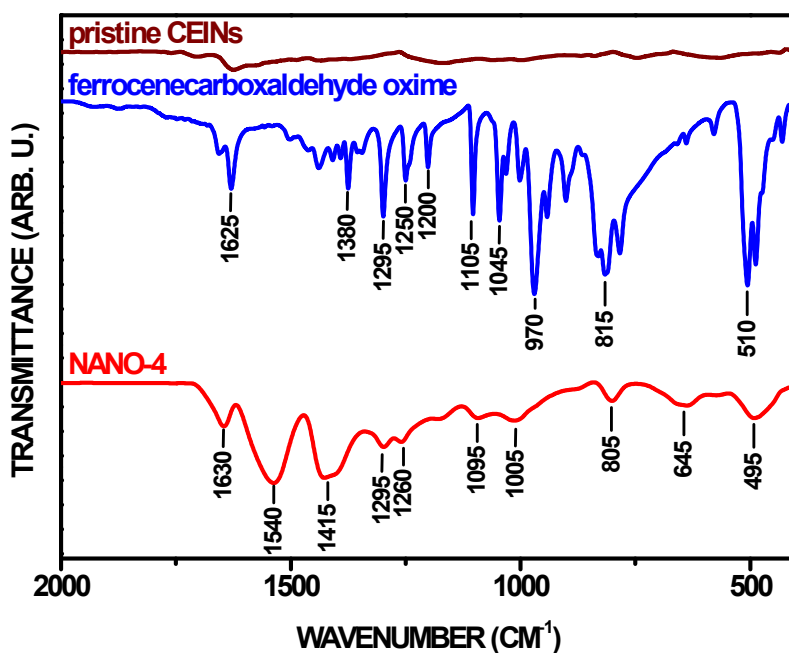
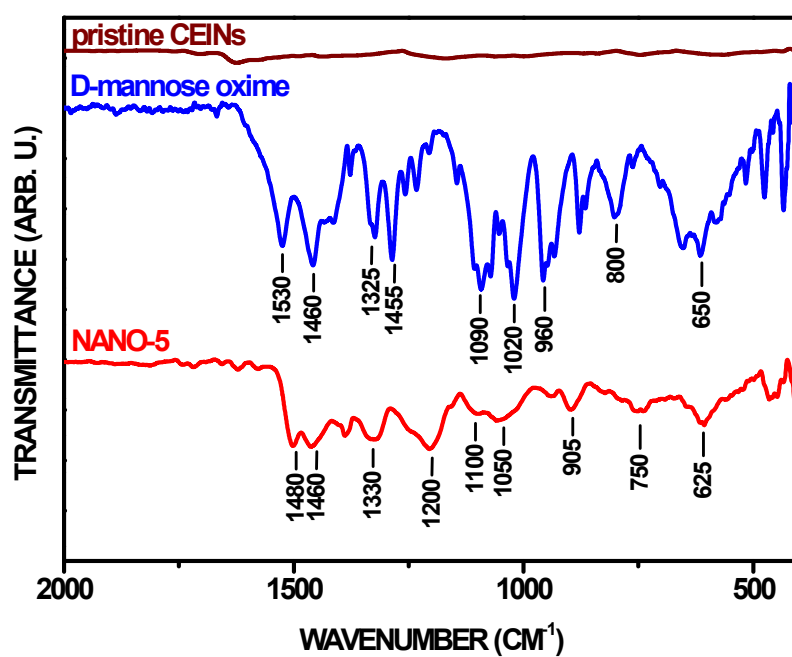


Fig. S18. FT-IR spectrum of NANO-4. FT-IR spectra of pristine CEINs and ferrocenecarboxaldehyde oxime are also presented. For legends see subsection 1.3 in ESI



**Fig. S19.** FT-IR spectrum of NANO-5. FT-IR spectra of pristine CEINs and D-mannose oxime are also presented. For legends see subsection 1.3 in ESI

#### 4. TGA curves

Thermal decomposition (under inert atmosphere) of a sugar and a metallocene results in the formation of char and metallic Fe, respectively. Therefore, for a proper calculation of the functionalization yield, char formation yields for D-mannose oxime and ferrocenecarboxaldehyde oxime need to be known. Char formation yield for D-mannose oxime (20%) was calculated from the data in Fig. S23. Char formation yield for ferrocenecarboxaldehyde oxime (52%) was reported earlier.<sup>4</sup>

For NANO-4 and NANO-5, because of the char formation coming from the introduced moiety, functionalization yield was calculated as follows<sup>5</sup>:  $C_F = (WL_{550} - M) \cdot (100\% - CH)$ , where  $C_F$  is the content of introduced organic moiety [%],  $WL_{550}$  is the observed weight loss up to 550°C,  $M$  is a content of moisture in the sample (weight loss up to 120°C),  $CH$  – char formation yield coming from the introduced moiety. For the other samples, i.e. NANO-1,2,3, content of the introduced organic moiety was calculated as follows:  $C_F = (WL_{550} - M)$ , because no char formation is observed for the introduced moiety.

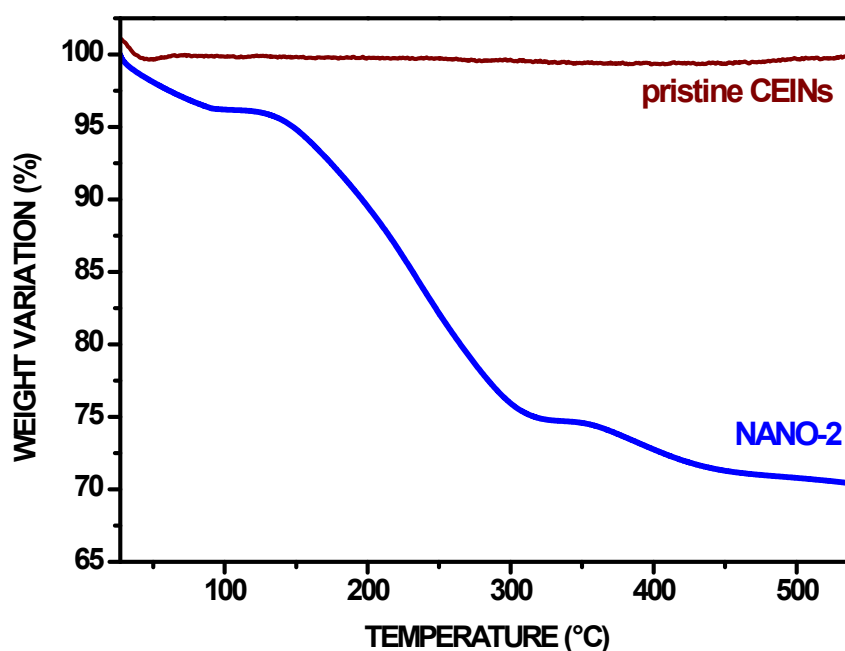


**Fig. S20.** TGA curve (in nitrogen) of NANO-2. TGA curve of pristine CEINs is also presented. For the legends see subsection 1.3 in ESI

<sup>4</sup> J.-H. Chai and Q.-S. Wu, *Beilstein J. Nanotechnol.*, 2013, **4**, 189–197.

<sup>5</sup> (a) M. Poplawska, M. Bystrzejewski, I. P. Grudzinski, M. A. Cywinska, J. Ostapko and A. Cieszanowski, *Carbon*, **2014**, *74*, 180-194; (b) A. Kasprzak, M. Poplawska, M. Bystrzejewski and I. P. Grudzinski, *J. Mater. Chem. B*, **2016**, *4*, 5593.

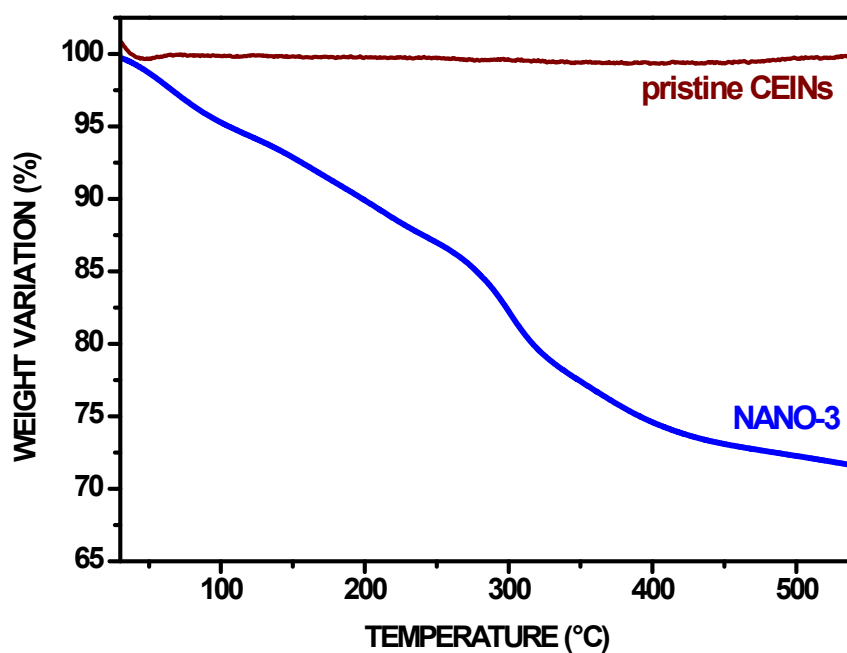


**Fig. S21.** TGA curve (in nitrogen) of NANO-3. TGA curve of pristine CEINs is also presented. For the legends see subsection 1.3 in ESI

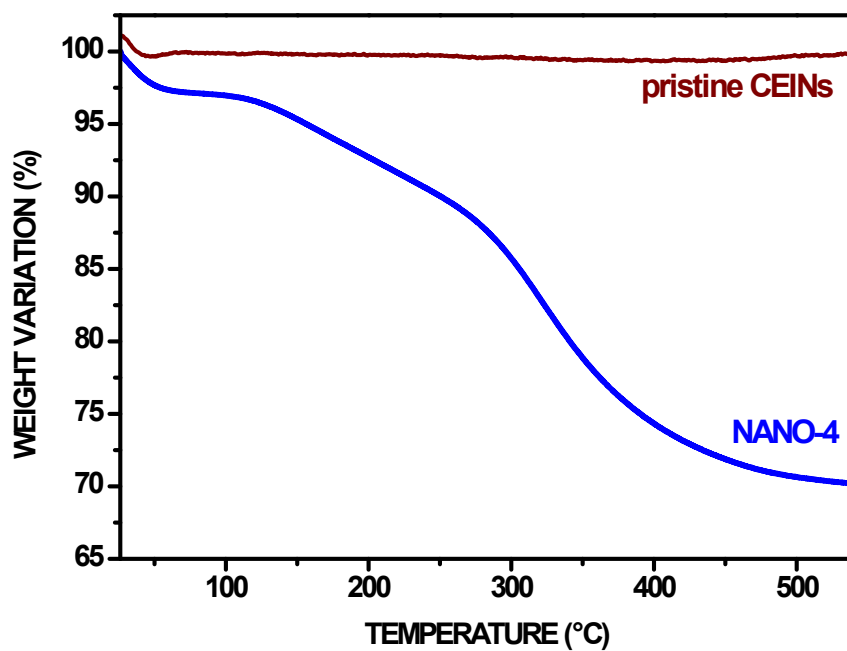


**Fig. S22.** TGA curve (in nitrogen) of NANO-4. TGA curve of pristine CEINs is also presented. For the legends see subsection 1.3 in ESI

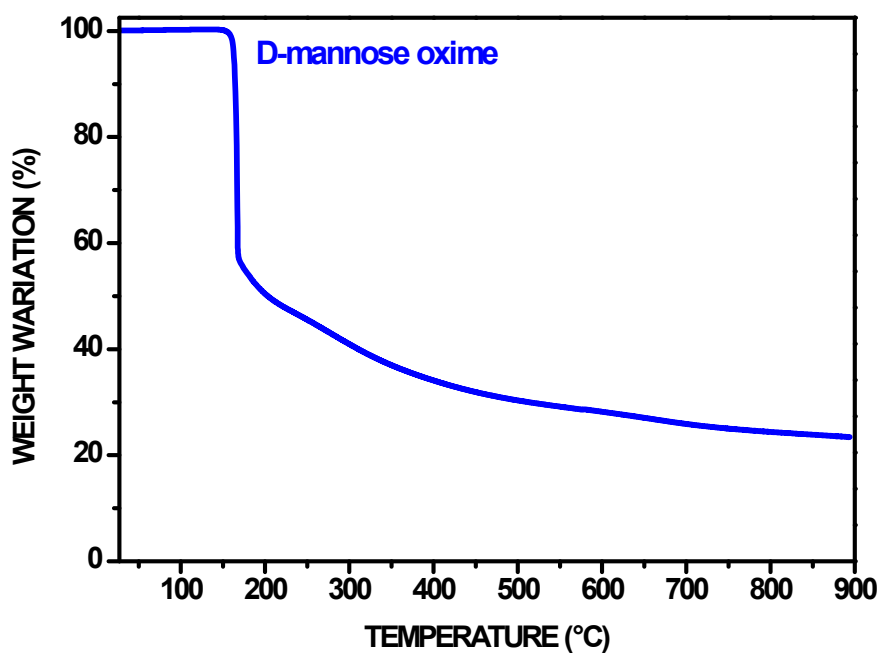


Fig. S23. TGA curve (in nitrogen) of D-mannose oxime

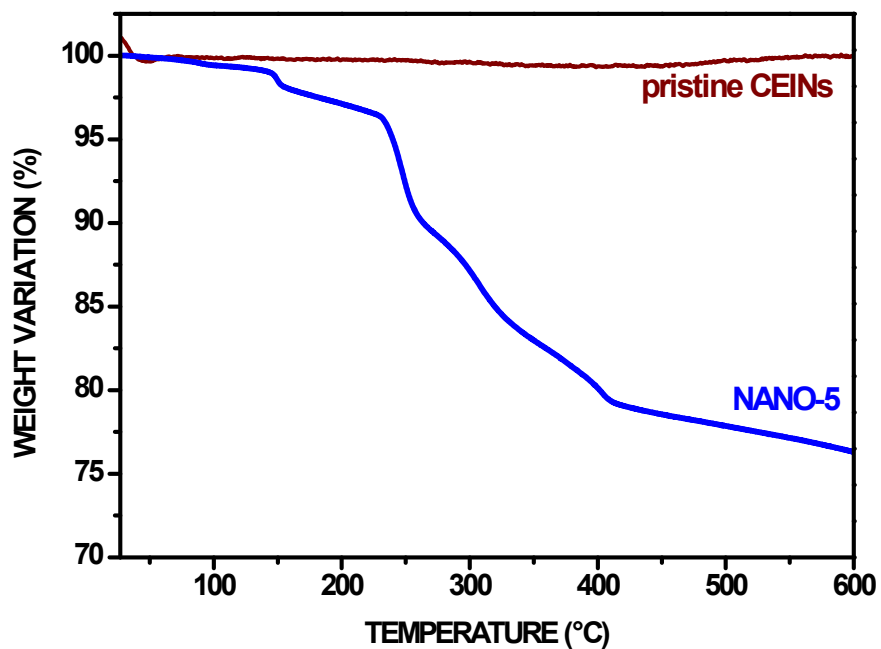


Fig. S24. TGA curve (in nitrogen) of NANO-5. TGA curve of pristine CEINs is also presented. For the legends see subsection 1.3 in ESI

## 5. XPS analyses – survey spectra

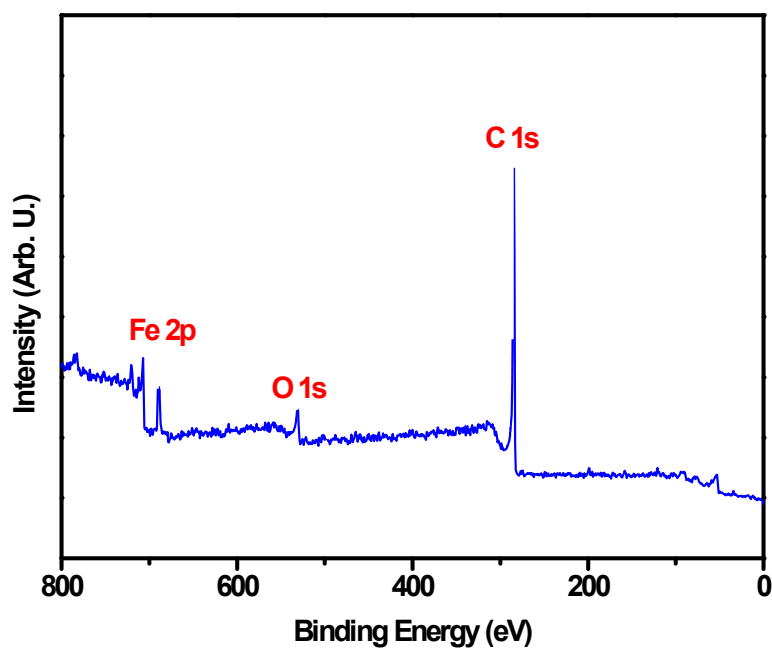


Fig. S25. Survey XPS spectrum for pristine CEINs

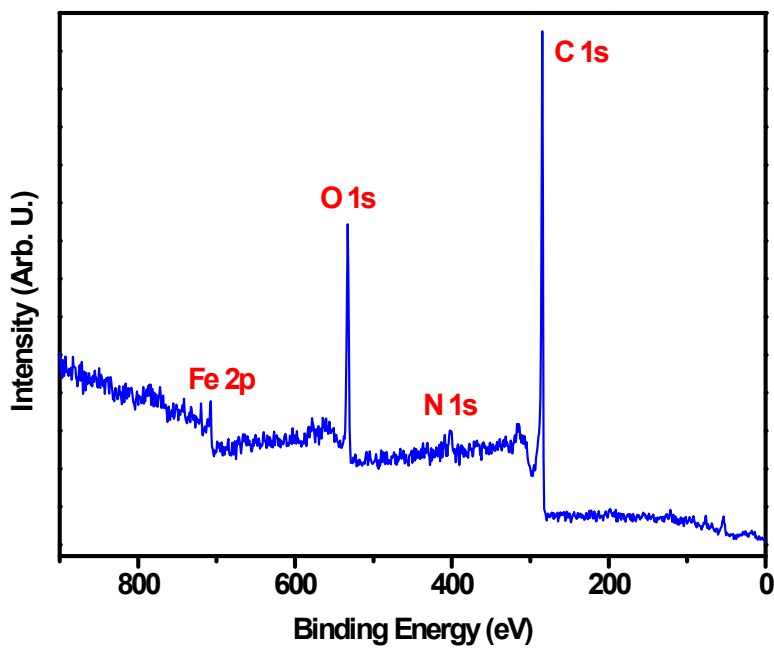


Fig. S26. Survey XPS spectrum for NANO-1. For the legends see subsection 1.3 in ESI

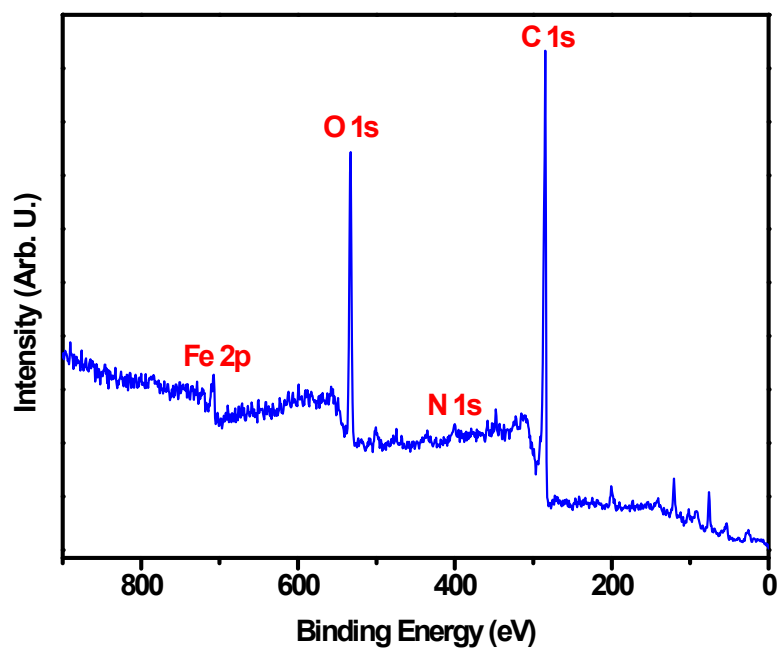


Fig. S27. Survey XPS spectrum for NANO-2. For the legends see subsection 1.3 in ESI

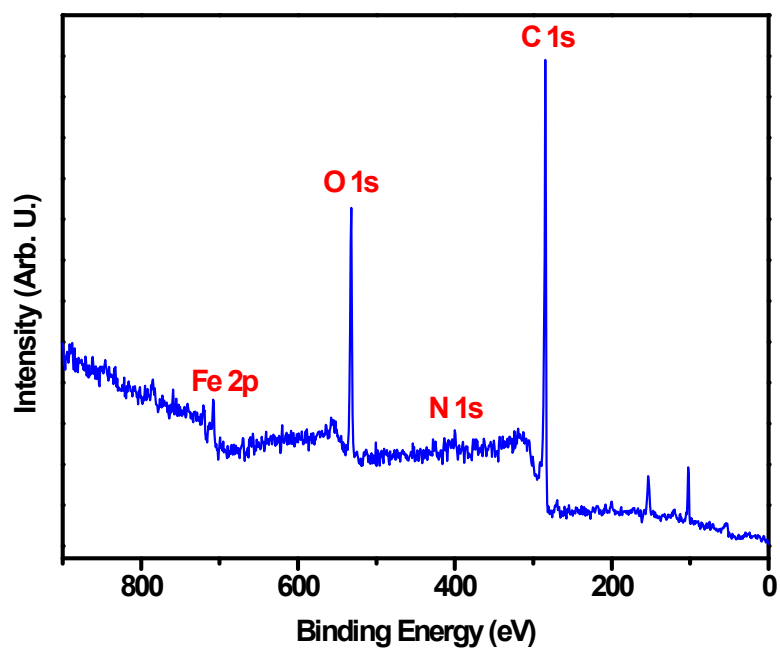
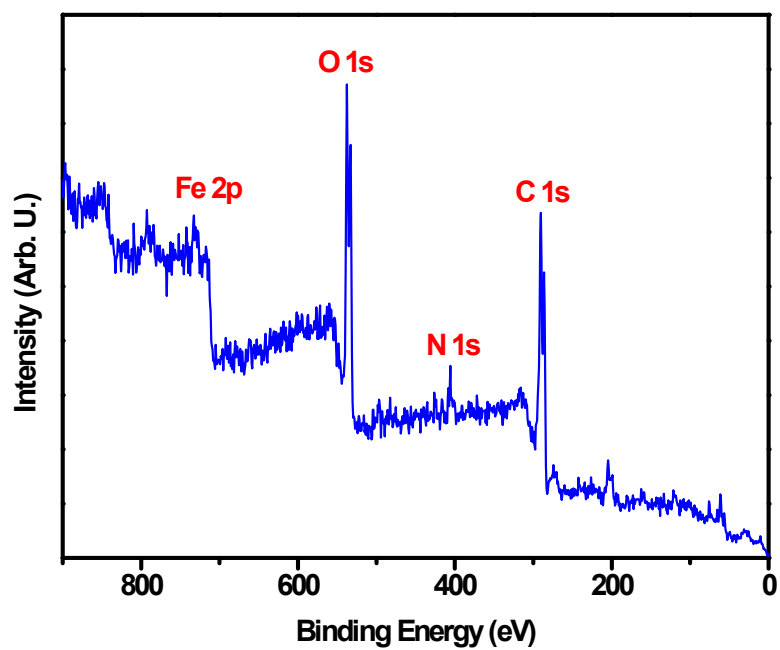
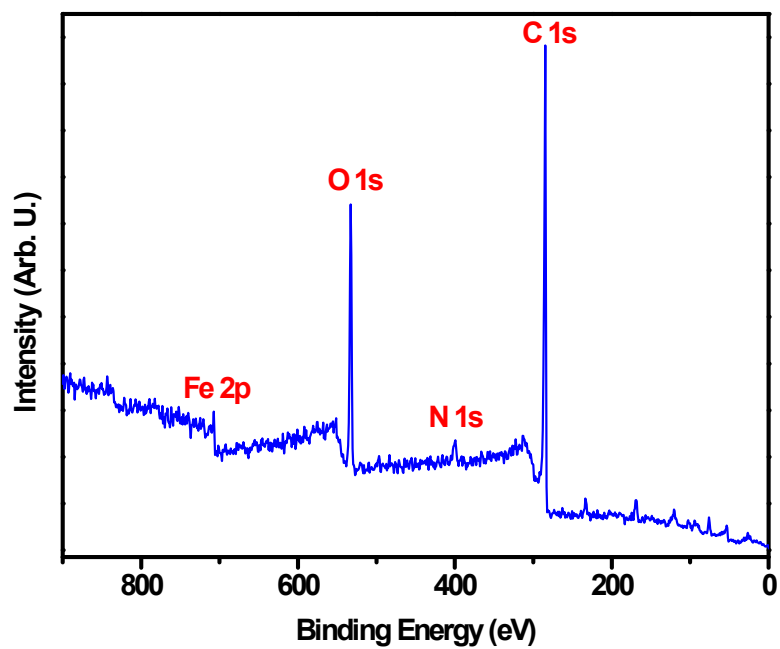


Fig. S28. Survey XPS spectrum for NANO-3. For the legends see subsection 1.3 in ESI



**Fig. S29.** Survey XPS spectrum for NANO-4. For the legends see subsection 1.3 in ESI



**Fig. S30.** Survey XPS spectrum for NANO-5. For the legends see subsection 1.3 in ESI

## 6. TEM images

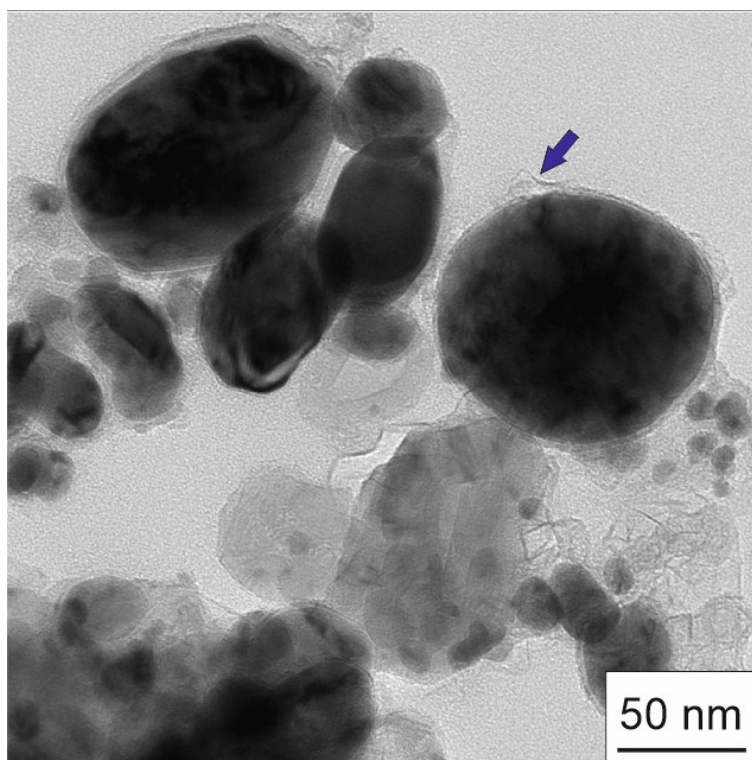


**Fig. S31.** Representative TEM image of NANO-2. For the legends see subsection 1.3 in ESI

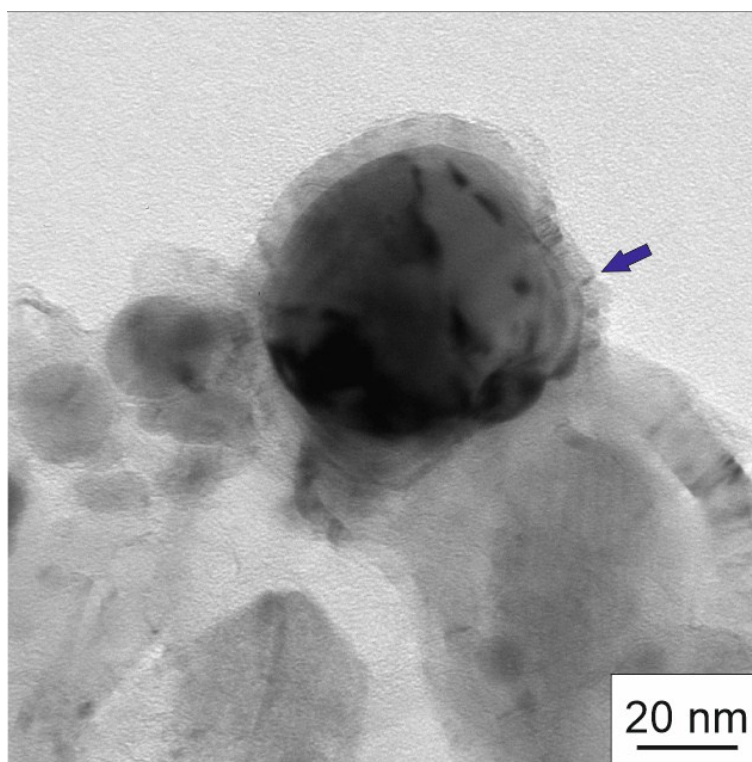


**Fig. S32.** Representative TEM image of NANO-3. For the legends see subsection 1.3 in ESI

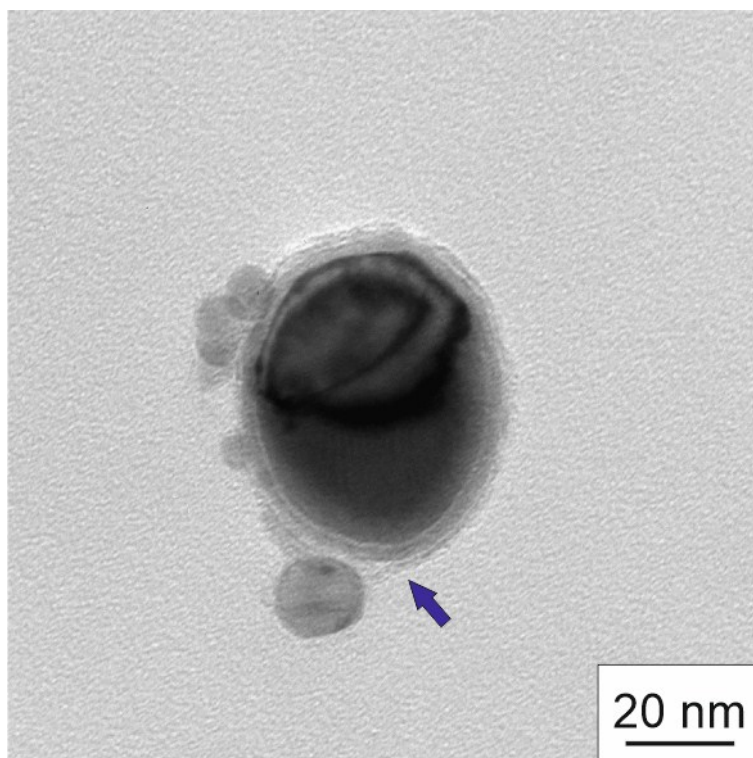


**Fig. S33.** Representative TEM image of NANO-4. For the legends see subsection 1.3 in ESI

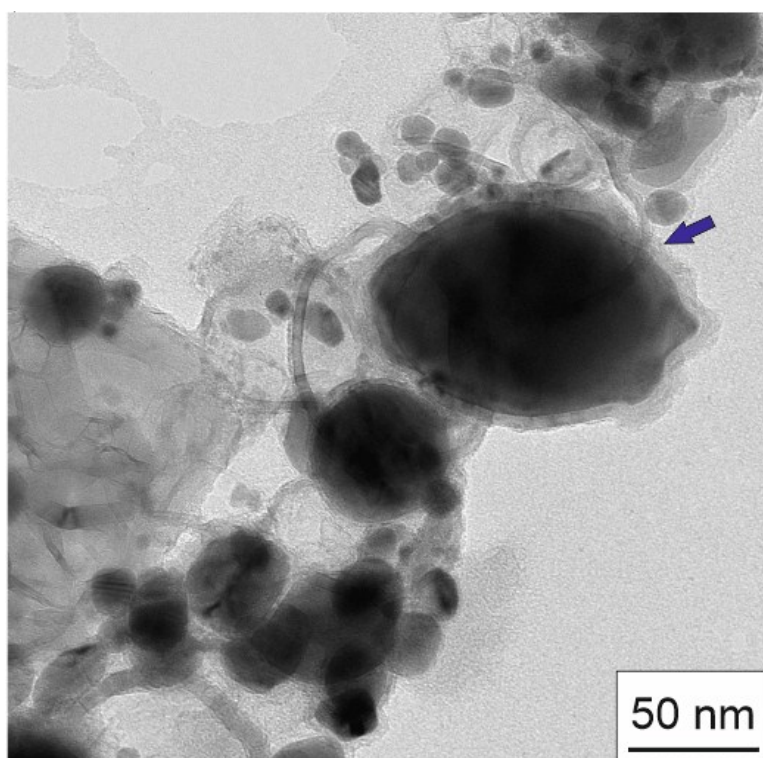


**Fig. S34.** Representative TEM image of NANO-5. For the legends see subsection 1.3 in ESI